Dyes and Pigments 88 (2011) 280–289

Contents lists available at ScienceDirect

Dyes and Pigments

journal homepage: www.elsevier.com/locate/dyepig

The synthesis and characterization of novel mesomorphic octa- and tetra-alkylthio-substituted lead phthalocyanines and their films

Devrim Atilla [a], Ayşe Gül Gürek [a], Tamara V. Basova [b,*], Vitaly G. Kiselev [c,d], Aseel Hassan [e], Liliya A. Sheludyakova [b], Vefa Ahsen [a,f]

[a] Gebze Institute of Technology, Department of Chemistry, P.O. Box: 141, 41400, Gebze, Kocaeli, Turkey
[b] Nikolaev Institute of Inorganic Chemistry, SB RAS, 3 Lavrentiev Ave., Novosibirsk 630090, Russia
[c] Institute of Chemical Kinetics and Combustion SB RAS, 3 Institutskaya Str., Novosibirsk 630090, Russia
[d] Novosibirsk State University, 2 Pirogova Str., Novosibirsk 630090, Russia
[e] Faculty of Arts, Computing, Engineering and Sciences, Sheffield Hallam University, Furnival Building, 153 Arundel Street, Sheffield S1 2NU, United Kingdom
[f] TUBITAK-Marmara Research Center, Materials Institute, P.O. Box: 21, 41470, Gebze, Kocaeli, Turkey

ARTICLE INFO

Article history:
Received 19 May 2010
Received in revised form
12 July 2010
Accepted 16 July 2010
Available online 27 July 2010

Keywords:
Lead phthalocyanines
Liquid crystals
IR spectroscopy
Thin films

ABSTRACT

Two novel mesomorphic octakis and tetrakis (alkylthio)-substituted phthalocyanines of Pb(II) were synthesized and characterized using NMR, UV–Vis, FT-IR and mass-spectrometry. The mesogenic properties of these new materials forming columnar-hexagonal mesophases were studied by differential scanning calorimetry, optical microscopy and X-ray diffraction. Visible absorption spectroscopy provided evidence of thermally induced molecular reorganization in films. IR spectroscopy and density functional theory calculations were used to study the preferential orientation of molecules relative to the substrate surface. The intense IR bands in the spectra of the lead phthalocyanines were assigned with the aid of quantum chemical computations. The observed increase in the intensity of the out-of-plane modes in the IR spectra correlate with an average preferential edge-on orientation of the molecules on the substrate surface in the film. The current-voltage characteristics of films before and after thermal treatment were also measured. The results confirmed the film ordering proposed on the basis of the IR and DFT studies.

1. Introduction

Metal phthalocyanines (MPcs) are highly stable organic semiconductors with a broad range of applications, such as light emitting diodes, solar cells, gas sensors, thin film transistors, and even single molecule devices [1]. Among the various MPcs, lead (Pb(II)) phthalocyanines are of particular interest due to their promising sensor [2,3] and electrical switching properties [4–6]. While an unsubstituted PbPc compound has attracted attention for a long time [7–13], only a few substituted PbPcs have been synthesized and characterized. Among the examples of those PbPc derivatives are the non-peripheral 1,4,8,11,15,18,22,25-octakis(hexylsulfanyl)Pc [14], non-peripheral tetraalkoxy-[15], tetra- and octa-diethoxymalonyle [16], cumylphenoxy- [17], tetranitro- [18], tetraamino- [19], and tetra-*tert*-butyl [20] derivatives. The structure of single crystals of $Pb[Pc(SC_6H_{13})_8]$ and $Pb[Pc(OC_5H_{11})_4]$ with substituents in non-peripheral positions were characterized by X-ray diffraction [14,15]. Non-linear optical properties of tetra-*tert*-butylnaphthalocyanine lead were also studied [20]. Density functional theory (DFT) calculations were applied to obtain molecular structures, HOMO–LUMO energy gaps, atomic charges, vibrational and UV–vis spectra of unsubstituted PbPc [21–23] and of some substituted $PbPcR_8$ compounds (R = F, Cl, Br, H, $-CH_3$, $-C_2H_5$, $-C_3H_7$) [21], $Pb[Pc(OC_2H_5)_4]$ [23], and $Pb[Pc(OC_5H_{11})_4]$ [23]. However, to our knowledge, no assignment of the IR bands in the spectra of substituted PbPcs has been made so far.

A very promising and fascinating class of PbPc compounds is *mesomorphic* lead phthalocyanines. The first successful synthesis of such species was reported in 1987 [24,25]. Simon et al. [24] showed that alkoxymethyl substituted phthalocyaninato lead(II) complexes ($PbPcR_8$, R = $-CH_2OC_nH_{2n+1}$; n = 8, 12) formed a hexagonal columnar mesophase which was stable at room temperature. Ford et al. [26] subsequently found that octa-(2-ethylhexyloxy) lead phthalocyanine exists in a mesophase in the temperature range from −100 °C to +200 °C. Compounds with $-CH_2OR$ and $-CH_2CH_2OR$ side chains turned out to be columnar liquid crystals with no detectable order within the columns [24,26]. An intramolecular antiferroelectric coupling of the molecules along the

* Corresponding author. Tel.: +7 383 330 28 14; fax: +7 383 330 94 89.
E-mail address: basova@niic.nsc.ru (T.V. Basova).

0143-7208/$ – see front matter © 2010 Elsevier Ltd. All rights reserved.
doi:10.1016/j.dyepig.2010.07.007

columns was found in Pb[Pc($CH_3(CH_2)_7OCH_2)_8$] [27] while the −OR side group yielded mesophases with some degree of intercolumnar organization [28]. Both the crystal-to-mesophase and the mesophase-to-isotropic phase transition temperatures were found to be lower for shorter paraffinic chains [29]. In comparison with other mesogen metalleted Pcs, Pb(II) destabilizes sterically the cofacial columnar structure and dramatically reduces both crystal-to-mesophase and mesophase-to-isotropic transition temperatures [30]. The strong dependence of the type of mesophase and the transition temperature on the nature of connecting link between the side chains and aromatic core was also observed [31,32].

Alkylthio-substituted PbPc derivatives have also attracted attention, mainly owing to better electroconductivity in comparison with alkyl and alkoxy analogues. Adam et al. [33] have shown that the highly ordered columnar phase of 2,3,6,7,10,11,13,14-hexahexylthiotriphenylene molecules exhibited an extraordinary high mobility of photoinduced charge carriers. However, only two examples of successful synthesis and characterization of *mesomorphic alkylthio-substituted PbPcs* have been reported so far by some of our co-workers [34]. In comparison with their Ni(II) and metal-free derivatives, mesomorphic alkylthio-substituted PbPcs possess lower clearing point temperatures [35,36].

The present contribution addresses the synthesis and characterization of new octa- and tetra-alkylthio-substituted lead phthalocyanines (**Pc1** and **Pc2**, Fig. 1). The mesogenic properties of these new materials were studied by differential scanning calorimetry, optical microscopy and X-ray diffraction. The preparation of thin films of these derivatives and their investigation by the UV–Vis absorption and IR spectroscopy techniques are also reported. Experimental studies were supported by theoretical considerations using quantum chemical (DFT) calculations for the detailed assignment of different bands in IR spectra of the lead phthalocyanines.

2. Experimental

2.1. Materials

4-(*n*-Hexadecylthio) phthalonitrile [37] and 4,5-Di(*n*-hexadecylthio) phthalonitrile [38] were synthesized according to the reported procedures. All other reagents and solvents of reagent-grade quality were obtained from commercial suppliers and were dried as described in Perrin and Armarego [39].

2.2. Measurements

Thermo Finnigan Flash 1112 was used for elemental analysis of all compounds under study. Infrared spectra in KBr pellets were recorded by a Bio-Rad FTS 175C FT-IR spectrophotometer. Optical spectra in UV–visible region were recorded with a UV-vis-3101PC "Shimadzu" using 1 cm pathlength cuvette at room temperature. Matrix-assisted laser desorption/ionisation time-of-flight mass-spectrometry (MALDI-TOF-MS) measurements were performed on a Bruker Daltonics micrOTOF (Bremen, Germany). Positive ion and linear mode MALDI-TOF-MS spectrum of **Pc1** and **Pc2** were obtained in 2,5-dihydroxy- benzoic acid MALDI matrix using nitrogen laser accumulating 50 laser shots. The phase transition behaviour of **Pc1** and **Pc2** was observed by means of a polarizing microscope (Leitz Wetzler Orthoplan-pol.) equipped with a hot stage (Linkam TMS 93) and a temperature controller (Linkam LNP). Transition temperatures were determined at a scan rate of 10 °C min^{-1} by using a Mettler Toledo Star Thermal Analysis System/DSC 822. Differential scanning calorimeter system was calibrated with 3 mg indium samples under nitrogen atmosphere. X-ray diffraction measurements (Cu-Kα-radiation) were performed using a Bruker Advanced D8 diffractometer. ^1H and ^{13}C NMR spectra were recorded in $CDCl_3$ solutions on a Varian 500 MHz spectrometer.

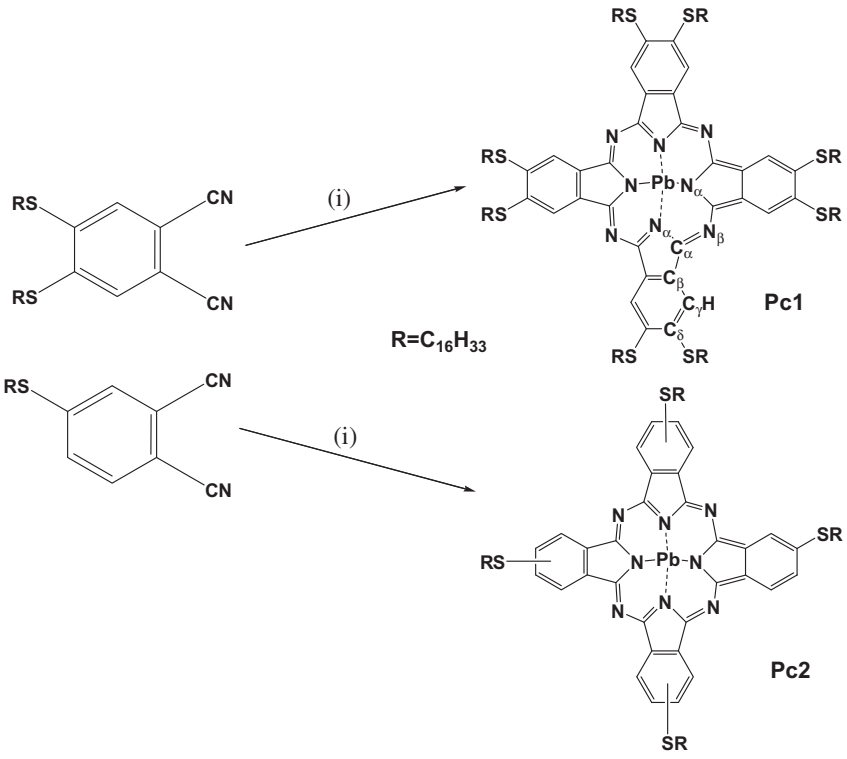

Fig. 1. Synthetic pathway and structure of **Pc1** and **Pc2** derivatives. (i) Pb(II)O and heating.

2.3. Synthesis

2.3.1. Octakis(n-hexadecylthio) Phthalocyaninato lead (II) (**Pc1**)

A round-bottomed flask fitted with a condenser was degassed and flame-dried under dry argon. The flask was charged under argon with 4,5-(*n*-hexadecylthio) phthalonitrile (0.369 g, 0.576 mmol) and anhydrous Pb(II)O (0.064 g, 0.288 mmol). The mixture was heated at 210 °C with stirring under argon atmosphere for 5 h without solvent. The reaction mixture was dissolved in chloroform, centrifuged, and the precipitate including inorganic impurities was removed. The solvent was evaporated and a crude product was passed through a Bio Beads column (Bio-Rad Laboratories) using CH_2Cl_2 as an eluent for eliminating organic impurities. This purification step was repeated two times. Purification was further achieved by preparative thin layer chromatography [silica gel; eluent CH_2Cl_2/n-hexane, 10:1 (v/v)]. Yield: 75 mg (19%). Anal. Calc. for $C_{160}H_{272}N_8PbS_8$: C, 69.33; H 9.89; N 4.04. Found C, 69.50; H, 9.43; N, 4.25. IR (KBr) ν_{max} (cm^{-1}) 2923, 2852, 1591, 1466, 1405, 1365, 1340, 1201, 1065. MS (MALDI-TOF) *m/z*, % (Fig. S1 in the Supplementary Information): 2774 $[M+H]^+$ (100). ^1H NMR {500 MHz, $CDCl_3$, δ (ppm)} (Fig. S2 in the Supporting Information): 0.90 (t, 24H, J = 6.94 Hz, CH_3), 1.26 (m, 192H, CH_2), 1.66 (m, 16H, CH_2), 1.94 (m, 16H, CH_2), 3.37 (t, 16H, J = 6.44 Hz, SCH_2), 8.99 (s, 8H, CH_{ar}). ^{13}C NMR {125 MHz, $CDCl_3$, δ (ppm)} (Fig. S3 in the Supplementary Information) 14.37 (CH_3), 22.94 (CH_2), 29.07–30.07 (CH_2), 32.19 ($SCH_2\underline{C}H_2$), 34.24 (SCH_2), 121.34 ($C_{ar}H$), 135.30(C_{ar}), 140.44 (C_{ar}), 153.84 ($C_{ar}\underline{C}_{\alpha}$=N).

2.3.2. Tetrakis (n-hexadecylthio)Phthalocyaninato lead (II) (**Pc2**)

Pc2 was prepared by the same procedure as described for **Pc1** starting with 4-(*n*-hexadecylthio) phthalonitrile (0.151 g, 0.394 mmol) and anhydrous Pb(II)O (0.043 g, 0.197 mmol). The reaction mixture was dissolved in chloroform, centrifuged, and a precipitate including inorganic impurities were removed. The solvent was evaporated and the crude product was passed through a Bio Beads column using CH_2Cl_2 as an eluent for eliminating organic impurities. The product was further purified with the preparative thin layer chromatography [silica gel; eluent CH_2Cl_2/n-hexane, 20:1 (v/v)]. A mixture of four peripherally substituted isomers of **Pc2** (each alkyl group has two possible substituting positions, Fig. 1) was synthesized. A separation of these isomers was not carried out. Yield: 45 mg (26%). Anal. Calc. for $C_{96}H_{144}N_8PbS_4$: 66.05; H 8.31; N 6.42. Found C, 66.10; H, 8.35; N, 6.53. IR (KBr) ν_{max} (cm^{-1}) 2954, 2921, 2850, 1598, 1467, 1384, 1315, 1143, 1079. MS (MALDI-TOF), *m/z*, % (Fig. S4 in the Supplementary Information): 1746 $[M+H]^+$ (100). ^1H NMR {500 MHz, $CDCl_3$, δ (ppm)} (Fig. S5 in the Supporting Information) 0.91 (t, 12H, CH_3, J = 6.66 Hz), 1.29 (m, 96H, CH_2), 1.64 (m, 8H, CH_2), 1.92 (m, 8H, CH_2), 3.27 (t, 8H, SCH_2), 7.80 (d, 4H, CH_{ar}, J = 7.85 Hz). 8.69 (m, 8H, CH_{ar}). ^{13}C NMR {125 MHz, $CDCl_3$, δ (ppm)} (Fig. S6 in the Supplementary Information): 13.10 (CH_3), 21.67 (CH_2), 28.05–28.74 (CH_2), 30.91 (CH_2), 32.38 (CH_2), 32.59 (SCH_2), 119.69 ($C_{ar}H$), 119.76 ($C_{ar}H$), 121.61 ($C_{ar}H$), 127.64 (C_{ar}), 133.11 (C_{ar}), 136.86(C_{ar}), 139.65 (C_{ar}), 152.88 ($C_{ar}C$ = N).

2.4. Quantum chemical calculations

The IR spectra of **Pc1** and **Pc2** were calculated at the B3LYP/LANL2DZ level of theory [40,41]. The geometries were fully optimized and each stationary point was fully characterized as a true minimum by the vibrational analysis. The vibrational frequencies were scaled by an empirically derived factor of 0.970. All calculations were performed using Gaussian 03 suite of programs [42].

2.5. Film preparation and characterization

Small amounts of solutions of **Pc1** and **Pc2** derivatives in THF (5 mg/ml) were dispensed by a glass pipette onto an ultrasonically cleaned substrate held onto photoresist spinner. The substrate was rotated for 60 s at a speed 2000 rpm. The solvent was evaporated upon rotation to generate a film of the phthalocyanine derivative. The substrates were varied according to the experimental requirements for different characterization.

Absorption spectra of the films on quartz substrates were recorded with a UV–visible scanning spectrophotometer (UV–vis-3101PC "Shimadzu") in the wavelength range 400–1200 nm. Infrared spectra of PbPcs in NaCl pellets and their films on NaCl substrates were recorded using Vertex 80 FT-IR spectrometer.

Current–voltage measurements were performed using a Keithley 6517A electrometer equipped with a microprocessor controlled measuring system. For the measurements of the in-plane film conductivity, the **Pc1** and **Pc2** films were spun onto glass substrates with inter-digitated electrodes (IDE) at an interelectrode distance L = 60 μm and at a width of electrode overlap W = 3.125 mm. All electrical measurements were performed in air at room temperature. Current–voltage dependencies were compared for the as-deposited and annealed films.

3. Results and discussion

3.1. Synthesis and general properties

The PbPc can be prepared by heating PbO or $Pb(OAc)_2$ with respective phthalonitrile derivative without solvent [16,17,26,34,43,44], or in *n*-pentanol [15]. Addition of anhydrous lead(II) acetate to a solution of Li_2Pc or H_2Pc in anhydrous alcohol also yields PbPc [15]. Apart from this, PbPc can be obtained by a microwave method [18,34]. In the present work, the cyclotetramerization of the dinitrile compounds was carried out in the presence of the dried PbO (Fig. 1) without any solvent according to the technique described in Refs. [16,17,34]. By the use of this method, we have already synthesized PbPcs with high yield comparable to the one of the earlier reported microwave procedure [34]. Therefore, we employed only the melting method to prepare the target PbPc compounds. The crude product was first passed through a Bio Beads column to eliminate organic impurities. Then the lead phthalocyanines obtained (**Pc1** and **Pc2**) were purified very quickly using preparative thin layer chromatography because the PbPcs transformed to corresponding metal-free analogues on a preparative TLC card. The chemical structures of **Pc1** and **Pc2** are shown in Fig. 1.

3.2. Spectroscopic characterization

The complexes **Pc1** and **Pc2** were characterized by elemental analysis and various spectroscopic methods. The mass spectra of the Pc compounds were obtained by means of MALDI-TOF-MS techniques. The protonated molecular ion peaks were observed, respectively, at 2774 $[M+H]^+$ and 1746 $[M+H]^+$. ^1H NMR spectra in $CDCl_3$ of the diamagnetic lead(II) compounds **Pc1** and **Pc2** were also recorded. Well-resolved multiplicity and integration of signals enabled an unambiguous assignment of the signals of all aliphatic protons.

The experimental IR spectra of **Pc1** and **Pc2** are presented in Fig. 2. Both phthalocyanine derivatives have a non-planar "shuttlecock" structure similar to unsubstituted lead phthalocyanine [7,45]. Small divalent ion complexes of phthalocyanines (Cu, Ni, Zn, Mg etc.) form planar complexes whereas larger ions (Pb, Sn) have too large radii (1.2 and 0.93 Å respectively) to fit the central cavity of the phthalocyanine ring. Due to this fact these ions lie out of the molecular plane of the phthalocyanine. The introduction of bulky alkyl substituents to the phthalocyanine ring leads to further distortion of Pc moiety; it becomes bent and the molecular

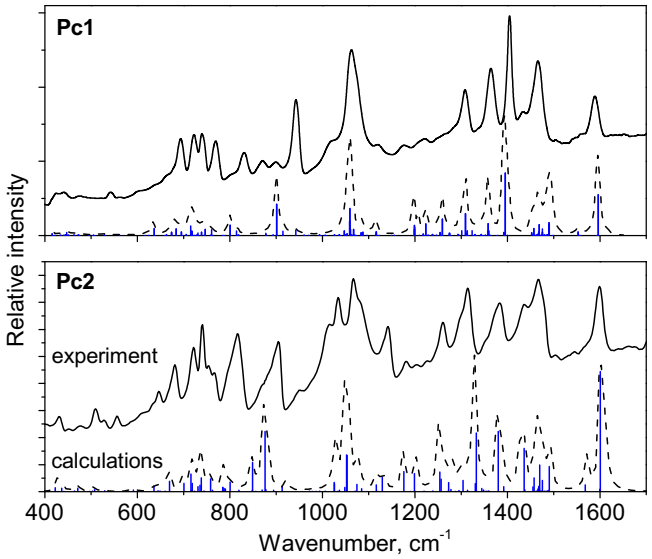

Fig. 2. The experimental (solid curves) and DFT-predicted (sticks) IR spectra of **Pc1** and **Pc2**. The calculated IR spectra were broadened by Lorentzians (dotted curves) of 5 cm^{-1} width.

symmetry reduces to C_4 for both **Pc1** and **Pc2** species. The alkyl chains in **Pc2** molecule are arranged parallel to the isoindole unit planes. Actually, a mixture of several isomers of **Pc2** with different positions of alkyl chains were synthesized (Fig. 1). However, all of them showed very similar spectral properties, therefore, only the IR spectra of 2,9,16,23- tetrakis(*n*-hexadecylthio)phthalocyaninato lead (II) were calculated. One of the alkyl chains in each benzene ring of **Pc1** molecule are also arranged parallel to isoindole unit plane, while the second one extends to the outside of the isoindole unit plane.

The fully optimized computed geometries of **Pc1** and **Pc2** are available in the Supporting Information (Table S1). Unfortunately, the experimental data on **Pc1** and **Pc2** crystal structure are not available (vide infra). Therefore, a comparison of the calculated bond lengths and bond angles of the studied compounds with the averaged experimental values of lead phthalocyanine analogues was made and the results are presented in Table 1. Apart from the computed values, Table 1 comprises X-ray crystallography data on unsubstituted monoclinic and triclinic PbPc [7,45], lead 1,4,8,11,15,18,22,25-octakis(hexylsulfanyl) phthalocyanine (PbPc(SC_6H_{13})$_8$) [14], and lead 1,8,15,22-tetrakis(3-pentyloxy) phthalocyanine (PbPc(α-OC_5H_{11})$_4$) [15]. It is seen from the Table 1 that the calculated bond lengths and angles of **Pc1** and **Pc2** are in good agreement with the corresponding values for other lead phthalocyanine derivatives. These results confirm the reliability of theoretical methods employed in the present work.

As was already mentioned, **Pc1** and **Pc2** belong to a C_4 molecular point group. All A and E modes are active in the IR spectra of these compounds. The calculated IR spectra of PbPc are also presented in Fig. 2. The assignment of experimental bands was primarily based on calculated spectra of PbPcs and on the IR intensity data. The comparison of experimental and calculated frequencies of the most intensive vibrations in the IR spectrum and their assignments are presented in Tables 2 and 3.

The experimentally measured vibrational frequencies of lead phthalocyanine molecules are in good agreement with the DFT theoretical predictions. The RMS difference between the calculated and experimental IR frequencies is 15 cm^{-1}.

The experimental IR spectrum in the range 400–1700 cm^{-1} is rather complicated (Fig. 2). The most part of intense peaks represent actually the mixture of several closely lying broadened vibrational modes. The most intensive peak in the predicted IR spectrum of **Pc2** corresponding to benzene stretching vibrations is located at 1600 cm^{-1} (Fig. 2, Table 3). Upon octa-substitution in **Pc1** this peak shifts to 1592 cm^{-1} and its relative intensity decreases in comparison with another band at 1404 cm^{-1} (1435 cm^{-1} for **Pc2**, Tables 2 and 3). This peak is mainly attributed to C–H deformations in benzene ring with some contribution of the benzene stretching vibrations (Table 2). Next intensive mode is located at 1063 and 1067 cm^{-1} for **Pc1** and **Pc2**, respectively (Fig. 2, Tables 2 and 3). The main contributions to the corresponding normal coordinates give ν(CC) and δ(CH_2) of alkyl substituents. Another important vibration corresponding to in-plane stretching vibrations of isoindole moiety lies at 943 cm^{-1} for **Pc1** (Table 2). The similar vibration in the spectrum of **Pc2** lies at 905 cm^{-1}, however, its normal coordinate also involves CH-deformations of benzene ring (Table 3).

It should be noted that the geometries and vibrational frequencies of **Pc1** and **Pc2** were calculated for a single molecule in the gas phase while the experimental IR spectra were measured in the solid state. It is therefore reasonable to expect that the conformations of the end alkyl groups in solid phthalocyanines might differ from the calculated ones. For example, the conformations of the hexyl groups of two molecules in the crystal cell of Pb[Pc(SC_6H_{13})$_8$] differ noticeably [14].

3.3. Mesogenic properties

The phase transition temperatures of **Pc1** and **Pc2** were determined by differential scanning calorimetry (DSC). DSC measurements were performed on the virgin materials with a scanning rate of 10 °C/min. Phase transition temperatures and the corresponding

Table 1
Experimental and theoretical bond lengths (Å) and bond angles (degrees) of various unsubstituted and substituted lead phthalocyanine derivatives. The atomic labels are given in accordance with Fig. 1.

	Experimental				Calculated		
	Monoclinic PbPc[a]	Triclinic PbPc[a]	Pb[Pc(OC_5H_{11})$_4$][b]	Pb[Pc(SC_6H_{13})$_8$][c]	Pb[Pc(OC_5H_{11})$_4$][d]	**Pc1**[e]	**Pc2**[e]
Pb–Nα	2.21	2.36	2.38	2.41	2.33	2.33	2.33
Nα–Cα	1.38	1.37	1.37	1.38	1.40	1.39	1.39
Cα–Cβ	1.49	1.46	1.46	1.46	1.47	1.47	1.47
Cγ–Cδ	1.44	1.40	1.39	1.40	1.42	1.41	1.41
Cδ–Cδ	1.38	1.40	1.38	1.38	1.41	1.44	1.43
Cδ–O			1.35		1.38		
Cδ–S				1.75		1.84	1.90
Nα–Pb–Nα	80	73.0	72.5	71.9	76.2	76.1	76.1
Cα–Nβ–Cα	120	124.2	122.9	124.0	125.6	125.2	125.2
Nα–Cα–Cβ	110	109.8	108.7	109.0	108.6	108.6	108.7

(a) Refs. [7,45] (b) Ref. [15] (c) Ref. [14] (d) Ref. [23] (e) This work.

Table 2
Experimental and calculated IR spectra of **Pc1** (cm^{-1}).

Experimental frequency	Calculated frequency	Symmetry irrep (C_4 group)	Intensity (arb. units)	Assignments
439	447	A	21	Cβ–Cγ–H OOP, Pb–Nα, Cα–Nα–Cα
509	636	E	45	Cβ–Cγ–Cδ, Cγ–Cδ–Cδ, Cα–Cβ–Cβ, Nβ–Cα–Nα
693	674	E	22	S–C_{alk}, δ(CC)$_{alk}$, Cα–Nα–Cα, Cβ–Cα–Nα
722	684	E	44	Cα–Nβ–Cα, Nα–Cα–Cβ, Pb–Nα, Cβ–Cβ–Cγ, S–C_{alk}
	695	E	23	S–C_{alk}, δ(CH_2)$_{alk}$ IP
740	715	A	65	δ(CH_2)$_{alk}$ torsional OOP
	716	E	32	δ(CH_2)$_{alk}$ torsional OOP
	718	A	29	δ(CH_2)$_{alk}$ torsional OOP
769	739	E	22	Cα–Nα–Cα, Nα–Cα–Nβ, Cα–Nβ–Cα, δ(CH_2)$_{alk}$, Cβ–Cγ–H
	747	E	41	Cα–Nβ–Cα, Nβ–Cα–Nβ, Cβ–Cβ–Cγ, Cγ–Cδ–Cδ, Cδ–S
	760	A	40	Cα-Nα-Cα, Cα-Nα, Cβ-Cγ-H, δ(CH_2)$_{alk}$ OOP
831	800	E	69	Cα–Nα–Cα, Cα–Nβ–Cα, Cβ–Cγ–Cδ, Cβ–Cγ–H
870	814	A	31	Cα–Nα–Cα, Pb–Nα, Cα–Nβ–Cα, Cβ–Cγ–Cδ
	878	A	15	δ(CH_3)$_{alk}$, δ(CC)$_{alk}$
943	901	E	210	Nα–Cα–Nβ, Cα–Nβ–Cα, Cδ–S, Cγ–Cδ–CδIP
	915	A	29	Cβ–Cγ–H OOP
	943	A	37	Cβ–Cγ–H, Cδ–Cγ–H OOP
1024	1047	E	30	Cα–Nα–Cα, Nα–Cα, Nα–Cα–Nβ, Cβ–Cγ–Cδ, ν(CC)$_{alk}$
1063	1058	E	96	ν(CC)$_{alk}$, δ(CH_2)$_{alk}$, Cβ–Cγ–H IP
	1059	E	182	Cβ–Cγ–H, Cδ–S, Cγ–Cδ–Cδ, δ(CH_2)$_{alk}$ IP
	1060	E	41	ν(CC)$_{alk}$, Cβ–Cγ–H, Cα–Nα
	1067	E	41	δ(CH_2)$_{alk}$, Cδ–Cγ–H
	1087	E	22	Cγ–Cδ–Cδ, Cγ–Cβ–Cβ, Cβ–Cγ–H, Cα–Nα, Cα–Nβ
	1116	E	26	δ(CC)$_{alk}$, δ(CH_3)$_{alk}$ OOP
	1116	A	20	ν(CC)$_{alk}$, δ(CH_2)$_{alk}$, δ(CH_3)$_{alk}$ OOP
1178	1199	E	68	δ(CH_2)$_{alk}$ IP
	1199	E	41	δ(CH_2)$_{alk}$ IP
	1200	A	54	δ(CH_2)$_{alk}$ IP
1219	1223	E	78	Cβ–Cγ–H, Cδ–Cγ–H, δ(CH_2)$_{alk}$ IP
	1254	E	21	δ(CH_2)$_{alk}$, Cβ–Cγ–H, Cα–Nα–Cα, Cα–Cβ, Nα–Cα
1282	1259	E	110	Cα–Nα–Cα, Nα–Cα, Nα–Cα–Nβ, Cα–Cβ, Cβ–Cγ–H, δ(CH_2)$_{alk}$
	1301	A	33	Cα–Nα–Cα, Nα–Cα, Cα–Nβ–Cα, Cβ–Cβ–Cα, Cβ–Cγ, Cα–Cβ, Cδ–Cδ
1308	1309	E	148	Cβ–Cβ, Cδ–Cδ–Cγ, Cβ–Cγ
	1313	E	31	δ(CH_2)$_{alk}$
	1323	A	31	Cα–Nβ–Cα, Nα–Cα, Cβ–Cβ–Cγ, Cβ–Cγ, Cδ–Cδ, Cδ–Cγ–H
1364	1358	E	79	Cδ–Cγ–H, Cα–Cβ–Cβ, Cα–Nβ, Cδ–Cδ
	1358	E	34	Cβ–Cγ–H, δ(CH_2)$_{alk}$ IP
	1359	E	32	δ(CH_2)$_{alk}$, Cβ–Cγ–H IP
	1392	E	20	δ(CH_3)$_{alk}$ OOP
1404	1395	E	421	Cδ–Cγ–H, Cγ–Cδ, Cα–Cβ IP
1434	1452	E	19	Cβ–Cγ–H, Cα–Nβ, Cα–Nα-Cα, Cγ–Cδ, δ(CH_2)$_{alk}$ OOP
	1457	E	47	δ(CH_2)$_{alk}$ OOP, Cα–Nβ
	1467	E	24	δ(CH_2)$_{alk}$ OOP
	1468	E	73	Cα-Nβ, Cβ–Cγ–Nα, Cα–Cβ, Cβ–Cβ, Cβ–Cγ–H, δ(CH_2)$_{alk}$
1465	1475	A	43	δ(CH_3)$_{alk}$ OOP
	1490	E	86	δ(CH_2)$_{alk}$ OOP
	1490	E	68	δ(CH_2)$_{alk}$ OOP
	1490	A	75	δ(CH_2)$_{alk}$ OOP
	1553	E	23	Cβ–Cβ, Cβ–Cγ, Cγ–Cδ, Cδ–Cδ
1588	1592	E	275	Cβ–Cγ, Cβ–Cβ, Cδ–Cδ

enthalpy changes of the PbPc complexes are summarized in Table 4. The DSC curves of both **Pc1** and **Pc2** have two significant peaks corresponding to liquid crystal phase transition and isotropic phase transition, respectively (see Table 4 and Figs. S7 and S8 in Supplementary Information).

To provide more detailed insight into the phase structure and phase transition of the studied compounds, we applied polarization microscopy technique. The birefringence textures were observed by polarizing optical microscopy while slowly cooling the sample from the isotropic phase to the mesophase. A photomicrograph of the mesophase of **Pc1** at 160 °C is shown in Fig. 3. A fan-shaped texture typical for Col_h mesophases was observed for both phthalocyanines. In mesogen metalleted Pcs, Pb(II) sterically destabilizes the cofacial columnar structure and reduces drastically both crystal-to-mesophase and mesophase-to-isotropic transition temperatures [30]. A decrease of clearing point temperatures was observed for **Pc1** in comparison with the metal-free phthalocyanine and Cu(II) derivatives [38]. It is also noteworthy that the clearing point of **Pc2** is lower than that of **Pc1** due to the fact that **Pc2** is actually a mixture of four isomers.

The identification of mesophases was carried out by X-ray diffraction measurements (Figs. S9 and S10 in the Supplementary Information). All X-ray diffraction data are summarized in Table 5. The mesophases were identified by microscopic observation and X-ray diffraction measurements at mesophase temperatures. The powder diffraction patterns of **Pc1** and **Pc2** contain typical reflections of a columnar mesophase of substituted Pcs [46]. In the low angle region, the phthalocyanine derivatives produce sharp peaks, the positions of which are in ratio $1:\sqrt{3}:\sqrt{4}:\sqrt{7}:\sqrt{9}$. These results suggest a two-dimensional hexagonal lattice with disk-like molecules stacked in columns in the hexagonal arrangement. In the large angle region the compounds **Pc1** and **Pc2** show a sharp peak

Table 3
Experimental and calculated IR spectra of **Pc2** (cm^{-1}).

Experimental frequency	Calculated frequency	Symmetry irrep (C_4 group)	Intensity (arb. units)	Assignments
430	422	E	15	Cα–Nβ–Cα, Nα–Pb, Cγ–Cδ–Cδ, Cδ–S–C_{alk}, Cδ–S
451	437	A	13	Cβ–Cγ–H OOP, Cδ–Cγ–H, Cα–Cβ–Cγ
509	471	A	13	Nβ–Cα–Nα, Cβ–Cγ–Cδ, Cβ–Cγ–H, Cγ–Cδ–H OOP
646	635	A	21	Cα–Nβ–Cα, Nα–Cα–Cβ,Cβ–Cγ–Cδ, Cδ–Cδ–S, Cδ–Cγ–H OOP
680	669	E	38	Cα–Nα–Cα, Pb–Nα, Cδ–S, Cβ–Cγ–Cδ IP
721	700	E	31	S–C_{alk} IP, $\delta(CC)_{alk}$
740	716	A	65	$\delta(CH_2)_{alk}$ torsional OOP
	719	A	30	$\delta(CH_2)_{alk}$ torsional OOP
	731	A	18	$\delta(CH_2)_{alk}$ torsional OOP
754	735	E	24	Cα–Nβ–Cα, Pb–Nα, Cα–Nα–Cα, Cβ–Cγ–Cδ, Cβ–Cγ–H OOP
	738	E	51	Cα–Nβ–Cα, Nβ–Cα–Nβ, Cβ–Cβ–Cγ, Cγ–Cδ–Cδ, Cδ–S
766	758	A	48	Cα–Nα–Cα, Pb–Nα, Cβ–Cγ–Cδ OOP
	785	E	16	Cβ–Cγ–H, Cβ–Cβ–Cγ, Cα–Nα–Cα, Pb–Nα, $\delta(CH_2)_{alk}$
	788	E	12	$\delta(CH_2)_{alk}$ torsional OOP, Cα–Nα–Cα, Cβ–Cγ–Cδ
816	800	A	36	Cα–Nα–Cα, Pb–Nα, Cα–Nβ–Cα, Cβ–Cγ–Cδ
870	850	A	108	Cγ–Cγ–H, Cδ–Cδ–H OOP
905	876	E	223	Nα–Cα–Nβ, Cα–Nβ–Cα, Cγ–Cδ–Cδ, Cδ–S, Cβ–Cγ–H IP
	912	A	21	Cβ–Cγ–H, Cδ–Cγ–H OOP
1034	1025	E	35	Cβ–Cγ–H, Cδ–Cδ–H, $\nu(CC)_{alk}$, $\delta(CC)_{alk}$, Cγ–Cδ–Cδ,
	1026	E	30	Cδ–Cγ–H, Cδ–Cδ–H, $\nu(CC)_{alk}$ IP
	1049	E	16	$\delta(CH)_{alk}$, $\nu(CC)_{alk}$ IP
1067	1053	E	136	$\nu(CC)_{alk}$, $\delta(CH_2)_{alk}$, Cβ–Cγ–H, Nα–Cα IP
	1054	E	133	$\nu(CC)_{alk}$, Cγ–Cδ–Cδ, Cβ–Cγ–H, Nα–Cα, Cα–Cβ–Cγ
1080	1075	E	27	Cδ–Cγ–H, Cγ–Cδ–H, Nα–Cα, Cβ–Cβ–Cγ, Cδ–S
	1084	E	11	$\nu(CC)_{alk}$, $\delta(CC)_{alk}$ IP
	1116	E	26	$\delta(CH_3)_{alk}$, $\delta(CC)_{alk}$
	1129	E	53	Cα–Nα–Cα, Cβ–Cβ–Cγ, Cγ–Cδ–Cδ, Cβ–Cβ, Cδ–Cγ–H, Cγ–Cδ–H OOP
1142	1177	E	74	Cδ–Cγ–H, Cγ–Cδ–H IP, Cα–Nα–Cα, Nβ–Cα
1180	1199	E	67	$\delta(CH_2)_{alk}$
1260	1254	E	73	Cδ–Cγ–H IP, Cα–Nα–Cα, Cα–Cβ, Nα–Cα, $\delta(CH)_{alk}$
	1256	E	47	$\delta(CH_2)_{alk}$ IP
1291	1273	E	33	Cδ–Cγ–H, Cδ–Cδ–H OOP, Nα–Cα
1300	1304	A	42	Nα–Cα, Cα–Cβ, Cα–Nβ–Cα, Nα–Cα–Nβ, Cβ–Cβ
	1330	E	30	$\delta(CH_2)_{alk}$, Cγ–Cδ
1315	1333	E	217	Cγ–Cδ, Cβ–Cγ, Cα–Cβ–Cβ, $\delta(CH)_{alk}$
1354	1345	E	12	$\delta(CH_2)_{alk}$
1383	1380	E	223	Cα–Nβ, Cβ–Cγ–H, Cδ–Cδ, Cδ–Cδ–H IP
	1391	E	19	$\delta(CH_3)_{alk}$
1435	1436	E	160	Cδ–Cδ–H IP, Cγ–Cδ, Cβ–Cγ, Cβ–Cβ–Cα
	1454	E	18	$\delta(CH_2)_{alk}$, Cγ–Cδ–H, Cβ–Cγ–H, Cβ–Cγ, Cα–Cβ
	1458	E	52	$\delta(CH_2)_{alk}$ OOP, Cα–Nβ
	1466	E	10	$\delta(CH_2)_{alk}$ OOP
	1468	E	20	$\delta(CH_2)_{alk}$ OOP
1467	1470	E	99	Cα–Nβ, Cα–Cβ, Cβ–Cβ, Cγ–Cδ, Cδ–Cγ–H, Cβ–Cγ–H IP
	1475	A	42	$\delta(CH_3)_{alk}$ OOP
1480	1490	E	93	$\delta(CH_2)_{alk}$
1544	1568	E	25	Cδ–Cδ, Cβ–Cβ, Cα–Cβ, Cα–Cβ–Cβ, Cδ–Cδ–H IP
1600	1600	E	444	Cδ–Cγ, Cβ–Cγ, Cα–Cβ

at 4.41 and 4.28 Å, respectively ($2\theta = 20°$). Most likely, this distance corresponds to paraffinic tails in the side chains. An additional reflection observed at ~3.5 Å ($2\theta = 25°$) for **Pc1** (but not for **Pc2**) may be assigned to packing macrocyclic subunits in the columns. A broad peak observed in the diffraction pattern of **Pc1** suggests the absence of long range translational disorder of the molecules along the axis of stacks. This fact is probably due to discotic hexagonal ordering of Col_{ho}-mesophase [46].

Table 4
Phase transition temperatures, °C (corresponding enthalpy changes in parentheses, kJ/mol) for the compounds **Pc1** and **Pc2** determined by DSC. Heating and cooling rates: 10 °C, heating range: −25–250 °C. Phase nomenclature: C – crystal, Col_h – discotic hexagonal columnar mesophase, I – isotropic phase.

	C → Col_h → I		I → Col_h → C	
	Heating		Cooling	
Pc1	31.2 [108.3]	204.5 [7.4]	184.7 [3.7]	22.8 [105.0]
Pc2	65.1 [24.9]	185.1 [6.3]	156.3 [7.0]	57.6 [23.7]

3.4. UV–Vis and IR spectroscopic studies of structural properties of films

Unfortunately, we were unable to grow crystals of appropriate quality for the X-ray diffraction studies. To bypass this obstacle, we applied optical spectroscopic techniques (viz., visible and IR spectroscopy) to obtain some information on the structure and ordering of PbPc films. In the following section we describe briefly the most important structural features of the films under different conditions.

The electronic absorption spectra of **Pc1** and **Pc2** solutions in tetrahydrofurane (THF) are presented in Fig. 4 (solid line). The spectra of solutions are characterized by an intense electronic absorption in the visible region, with the Q-band at 739 and 723 nm for **Pc1** and **Pc2**, respectively. The intense Q-bands are shifted to longer wavelengths in comparison with nickel and metal-free Pc analogues [21,38].

The lead phthalocyanines are often chemically unstable. Both the solution and the thin films of PbPcs are prone to the loss of the Pb^{2+} central ion forming metal-free phthalocyanine (H_2Pc) while

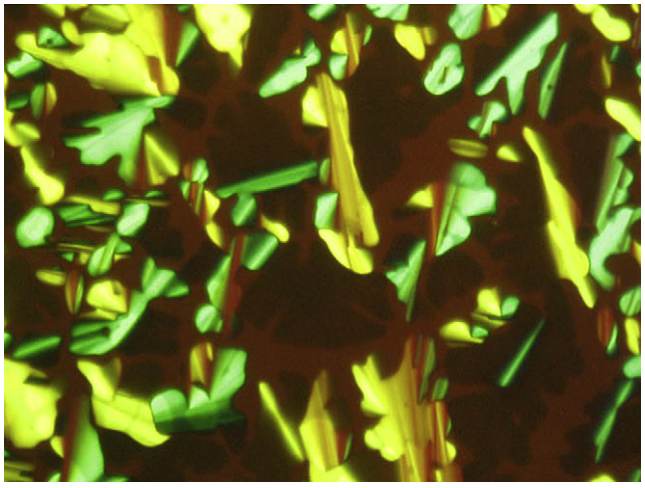

Fig. 3. The optical texture of the **Pc1** observed at 160 °C.

heated and even stored at room temperature [34]. On the contrary, the films of **Pc1** and **Pc2** are characterized by a higher stability and do not lose the metal atom at least for some weeks. To confirm the composition of the films before and after heating they were washed away from the substrate by THF and the electronic absorption spectra of the solutions were recorded. The spectra obtained were similar to the ones in Fig. 4a and b (solid lines). The split of the Q-band, which might indicate the formation of H_2Pc, was not observed in the spectra.

Fig. 4 (dashed line) shows the UV–Vis absorption spectra of the spun films of the phthalocyanines at room temperature immediately after deposition. A single optical absorption band corresponding to the HOMO-LUMO π–π transition splits into Q_x and Q_y components due to a reduction of molecular symmetry in the crystalline environment [47]. Note that the splitting of these bands correlate with the extent of distortion. As a consequence, the position and intensity of Q-band in the visible region are very sensitive to the specific crystalline phase.

In particular, the wide Q-band, ranging from about 650 to 1050 nm, is characterized by at least two components, Q_x (shorter wavelengths) and Q_y (longer wavelengths). The large splitting is observed for the films of **Pc1** and **Pc2** before heating (Fig. 4, dashed lines). The position of the Q_y bands, shifted to 979 nm in the case of **Pc1** and to 893 nm in the case of **Pc2**, is an indication of a lower

Table 5
X-Ray diffraction data for **Pc1** and **Pc2**.

	Observed spacings (Å)	Theoretical spacings (Å)	Lattice constant (Å)	Ratio	Miller indices
Pc1	25.97	25.97	a = 30.02	1	(100)
	15.01	14.99	Col_{ho} at 35 °C	√3	(110)
	12.97	12.98		√4	(200)
	9.85	9.81		√7	(210)
	8.65	8.66		√9	(300)
	7.50				
	6.32				
	4.41				
	3.51				
Pc2	22.09	22.09	a = 25.51	1	(100)
	12.73	12.75	Col_h at 70 °C	√3	(110)
	10.13	11.06		√4	(200)
	8.39	8.35		√7	(210)
	7.44	7.36		√9	(300)
	6.21				
	4.28				

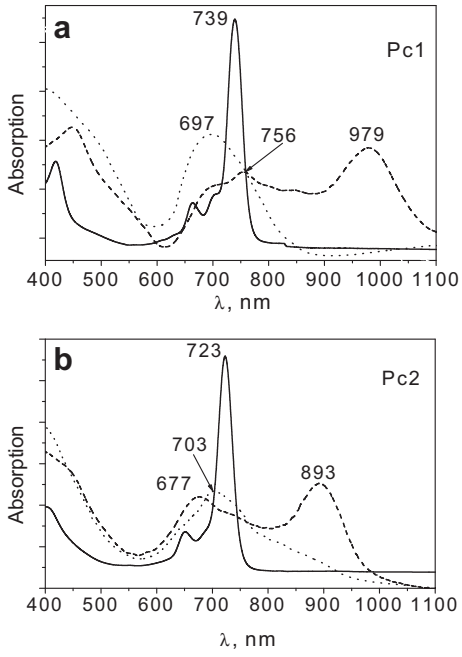

Fig. 4. The electronic absorption spectra of **Pc1** (a) and **Pc2** (b): a solution in THF (solid line); an as-deposited film on quartz (dashed line); a film on quartz after annealing at 220 °C (dotted line).

lattice contraction along the molecular stack. The spectrum of **Pc1** film is more complicated and contains other peaks at 756 and 850 nm that originate possibly from components of other phases. Such spectra with wide splitted Q-band are similar to those for triclinic phase of unsubstituted lead phthalocyanine [48] and for the crystalline phase II of TiOPc and VOPc [47,49].

Kasha et al. [50] proposed a simple model explaining how the orientation of transition dipole vectors of two interacting molecules influences the electronic spectra. The corresponding band splits only in the case of so-called oblique dimers (i.e., those with non-parallel alignment of dipole vectors). Other types of dimer alignment (parallel, co-planar and in-line) do not lead to splitting of bands. Therefore, according to the above proposed model [50], the split of Q-bands in the spectra of the films before heating refers to oblique (roof-top-shaped) dimers. A steady transformation of the films after heating to the temperature of isotropic liquid and then cooling down to the room temperature leads to a decrease in intensity of the longer wavelength bands. It is seen from Fig. 4(a) that the split Q-bands at 756 and 979 nm (dashed line) transform to a single band at 697 nm after heating of **Pc1** film (dotted line). This wide single Q-band in the spectrum may correspond to cofacial (face-to-face) or slipped (co-planar) dimers [51–53].

The temperature of liquid crystalline phase transition (cooling stage) of **Pc1** is 22.8 °C, therefore the room temperature (25 °C) state of this species is a liquid crystalline. The molecular layers in **Pc1** films most probably re-organize irreversibly such that the herring-bone columns transform into columns of fully cofacial molecules. This type of reorganization is analogous to that undergone by the octaalkyl analogues upon transition from the crystal phase to the hexagonal discotic mesophase [51,54,55].

The Q-band (703 nm) in the spectrum of the **Pc2** film after heating has a shoulder at about 745 nm (Fig. 4(b), red curve). The presence of this shoulder indicates the crystallization of **Pc2** at room temperature and formation of another crystalline phase upon heating.

The IR spectroscopy was used to study the preferential orientation of molecules relative to the substrate surface. The IR spectra

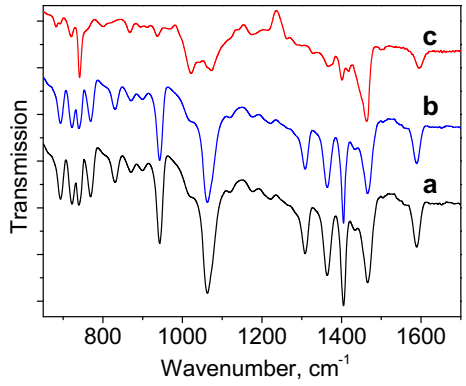

Fig. 5. The IR spectra of **Pc1**: (a) in a NaCl pellet; (b) an as-deposited **Pc1** film on NaCl substrate; (c) the same film after heating to 220 °C and cooling down to a room temperature.

of **Pc1** and **Pc2** in the NaCl pellet (black curve) and in the film deposited on NaCl surface (blue curves) are presented in Figs. 5 and 6, respectively. A comparison of the relative intensities of in-plane and out-of-plane modes in IR spectrum of NaCl pellet and films shows the extent of molecular organization and preferential orientation of molecules in the film [56,57].

As was mentioned above, the IR spectra of Pc1 and Pc2 are rather complicated because of the large number of overlapping modes belonging to the phthalocyanine ring and substituents. Nevertheless, some bands (namely, C–H out-of-plane and in-plane deformations, in-plane isoindole bending and stretching, vide infra) can still be used for the study of the film orientation. In NaCl pellet phthalocyanine molecules are distributed randomly without any preferred orientation (Fig. 5(a) and 6(a)), and the relative intensities of in-plane and out-of-plane modes would simply correspond to the transition dipole moment associated with a particular vibration. The spectra of the pellet and films of PbPcs before heating are very similar (Fig. 5(b) and 6(b)), indicating the absence of the preferable orientation of the phthalocyanine molecules on the substrate surface.

The IR spectra of the films of **Pc1** and **Pc2** after heating to the temperature of isotropic liquid and then cooling down to the room temperature are given in Fig. 5(c) and 6(c), respectively. It is seen that the relative intensities of some bands have decreased significantly. This is a clear indication of a certain degree of molecular organization in the film where the transition dipole moment vectors are partially aligned with respect to the substrate surface. Since the wave vector of the incident light is normal to this surface,

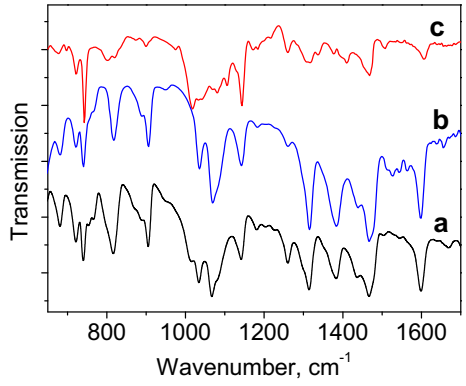

Fig. 6. The IR spectra of **Pc2**: (a) in a NaCl pellet; (b) an as-deposited **Pc2** film on NaCl substrate; (c) the same film after heating to 220 °C and cooling down to a room temperature.

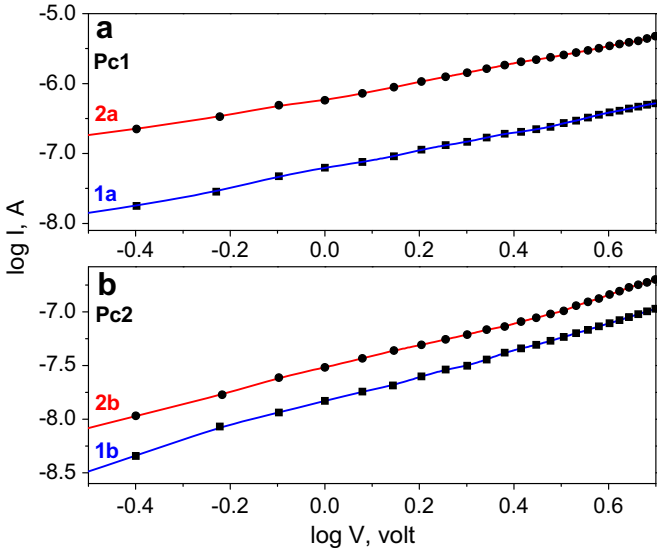

Fig. 7. The current–voltage characteristics of the **Pc1** (a) and **Pc2** (b) films deposited on an inter-digitated planar structure before (curves 1a, 1b) and after (curves 2a, 2b) thermal treatment in air. For clarity, the experimental points are fitted by a spline.

the *in-plane* modes would only be excited, and the *out-of-plane* modes should not be observed for a molecular orientation with a C_4 axis perpendicular to the surface (face-on). Correspondingly, an edge-on molecular orientation would result in an increase of the relative intensity of the out-of-plane vibrations. A significant difference of the spectra of pellet samples and of the films after annealing is especially pronounced for the A modes at 740 cm^{-1} (C–H out-of-plane deformations, Tables 1, 2). They become very prominent in the **Pc1** film spectra (Fig. 5(c)), while the intensities of some in-plane modes, e.g. the C–H deformation modes (1063, 1364 cm^{-1}), the in-plane isoindole bending (943 cm^{-1}) and stretching (1404 cm^{-1}) modes (Table 1) undergo a significant reduction. The enhancement of the intensity of the out-of-plane modes in the transmission spectrum correlate with an average preferential edge-on orientation of the phthalocyanine molecules on the substrate surface in **Pc2** film. Similar tendency is observed for **Pc1** films (Fig. 6(c)). We therefore infer that the new edge-on molecular orientation formed during the heating process remains largely unchanged in the cooled films of **Pc2**. Similar orientation of the molecules relative to the substrate surface was also observed for planar metal phthalocyanines deposited on the surface of one substrate with an air interface [55,58,59].

3.5. D.C. conductivity of *Pc1* and *Pc2* films

Current-voltage characteristics of **Pc1** and **Pc2** films deposited on inter-digitated planar electrode structures are given in Fig. 7(a) and 7(b), respectively, both before and after thermal treatment in air. When plotted in the log–log scale, the data for both films demonstrate ohmic conduction in the most part of the applied voltage range. A slight increase of the slope of the log I–log V plot is observed in the region of log $V > 0.5$ (~3 V, Fig. 7(a) and 7(b)) indicating the onset of a high field transport mechanism such as space charge limited conduction. The latter is expected to occur in low-conductivity materials at high applied fields [60].

The lateral d.c. conductivities ($\sigma_{//}$) are $4.5 \cdot 10^{-6}$ and $1.2 \cdot 10^{-5}$ Ω^{-1} m^{-1} for the as-deposited films of **Pc1** and **Pc2**, respectively, before thermal treatment. After the heating these values increased to $1.2 \cdot 10^{-5}$ and $1.8 \cdot 10^{-4}$ Ω^{-1} m^{-1} for **Pc1** and **Pc2**, respectively.

An increase of the lateral conductivity of the PbPc film upon heating may be explained by changing of the film organization: the initially disordered films of PbPc become ordered. The stacks of molecules are formed upon heating with the stacking axis parallel to the substrate surface. This result is also confirmed by the IR spectroscopy studies (cf. Section 3.4).

4. Conclusion

In this work, the synthesis of new mesomorphic octakis (alkylthio)-substituted phthalocyanines of Pb(II) have been described. The Pb(II) phthalocyanines were characterized using different spectroscopic techniques (NMR, UV–Vis, FT-IR, and Mass-spectrometry). The phase transition temperatures of the complexes have been determined by the polarization microscopy and DSC. The formation of the columnar-hexagonal (Col_h) mesophase over a wide temperature range was confirmed by X-ray phase analysis.

Thermally induced molecular reorganization within PbPc films was studied by visible absorption spectroscopy. The broadened and blue-shifted Q-bands in the visible absorption spectra of the films after heating provide an evidence of a molecular ordering and indicate a cofacial (face-to-face) arrangement of molecules in the films.

The IR spectroscopy was used to study the preferential orientation of molecules relative to the substrate surface. Quantum chemical (DFT) calculations were used for the detailed assignment of the IR bands in the spectra of the lead phthalocyanines. The enhancement of the intensity of the out-of-plane modes in the transmission IR spectra correlate with an average preferential edge-on orientation of the Pc molecules on the substrate surface in the film.

The current–voltage characteristics of PbPc films deposited on inter-digitated planar electrode structures were measured, both before and after thermal treatment. An increase of lateral conductivity of both **Pc1** and **Pc2** films upon heating agrees with the results of IR studies demonstrating preferential edge-on orientation of the Pc molecules in the film.

Acknowledgement

This work was supported by The Scientific & Technological Research Council of Turkey (TUBITAK)-108 M 384 Project and RFBR grant #09-03-91219. Support of this work by the Siberian Supercomputer Center is gratefully acknowledged. V.G.K. also appreciates the support of this work by the Russian Federal Agency of Education (project NK-187P(6), contract #P1475) and SB RAS (Lavrentiev grant programme).

Appendix. Supplementary material

Supplementary data associated with this article can be found, in the online version, at doi:10.1016/j.dyepig.2010.07.007.

References

[1] McKeown NB. The synthesis of symmetrical phthalocyanines. In: Kadish KM, Smith R, Guilard R, editors. Applications of phthalocyanines. The Porphyrin Handbook, vol. 15. San Diego, CA: Academic Press; 2003. p. 61–124.
[2] Campbell D, Collins RA. Spectral response of monoclinic and triclinic lead phthalocyanine to nitrogen dioxide. Thin Solid Films 1995;261:311–6.
[3] Shahrokhian S. Lead phthalocyanine as a selective carrier for preparation of a cysteine-selective electrode. Analytical Chemistry 2001;73:5972–8.
[4] Machida Y, Saito Y, Taomoto A, Nichogi K, Waragai K, Asakawa S. Japanese Journal of Applied Physics 1989;28:297–8.
[5] Ambily S, Menon CS. Electrical conductivity, optical absorption and structural studies of thin films of lead phthalocyanine. Materials Letters 1998;36:61–4.
[6] Mukherjee B, Ray AK, Sharma AK, Cook MJ, Chambrier I. A simply constructed lead phthalocyanine memory diode. Journal of Applied Physics 2008; 103:074507.
[7] Iyechika Y, Yakushi K, Ikemoto I, Kuroda H. Structure of lead phthalocyanine (triclinic form). Acta Crystallographica Section B 1982;38:766–70.
[8] Przyborowski F, Hamann C. The monoclinic modification of lead phthalocyanine – a Quasi-one-dimensional metal with characteristic order of molecular dipoles. Crystal Research and Technology 1982;17:1041–5.
[9] Bluhm TL, Wagner HJ, Loutfy RO. Unit cell parameters for a new crystalline polymorph of lead phthalocyanine and for two polymorphs of magnesium phthalocyanine. Journal of Materials Science Letters 1983;2:85–7.
[10] Collins RA, Krier A, Abass AK. Optical properties of lead phthalocyanine (PbPc) thin films. Thin Solid Films 1993;229:113–8.
[11] Ottaviano L, Lozzi L, Phani AR, Ciattoni A, Santucci S, Di Nardo S. Thermally induced phase transition in crystalline lead phthalocyanine films investigated by XRD and atomic force microscopy. Applied Surface Science 1998;136:81–6.
[12] Ambily S, Xavier FP, Menon CS. Photoconductivity measurements in lead phthalocyanine thin films. Materials Letters 1999;41:5–8.
[13] Papageorgiou N, Ferro Y, Salomon E, Allouche A, Layet JM, Giovanelli L, et al. Geometry and electronic structure of lead phthalocyanine: quantum calculations via density-functional theory and photoemission measurements. Physical Review B 2003;68:235105.
[14] Burnham PM, Cook MJ, Gerrard LA, Heeney MJ, Hughes DL. Structural characterisation of a red phthalocyanine. Chemical Communication; 2003:2064–5.
[15] Bian Y, Li L, Dou J, Cheng DYY, Li R, Ma C, et al. Synthesis, structure, spectroscopic properties, and eElectrochemistry of (1,8,15,22-tetrasubstituted phthalocyaninato) lead complexes. Inorganic Chemisrty 2004;43:7539–44.
[16] Dinçer HA, Çerlek H, Gül A, Koçak MB. Synthesis and spectral properties of tetra- and octa-substituted lead phthalocyanines. Main Group Chemistry 2005;4:209–12.
[17] Snow AW, Jarvis NL. Molecular association and monolayer formation of soluble phthalocyanine compounds. Molecular association and monolayer formation of soluble phthalocyanine compounds. Journal of the American Chemical Society 1984;106:4706–11.
[18] Achar BN, Kumar TMM, Lokesh KS. Journal of Porphyrins and Phthalocyanines 2005;9:872–9.
[19] Kumar TMM, Achar BN. Synthesis and characterization of lead phthalocyanine and its derivatives. Journal of Organometallic Chemistry 2006;691:331–6.
[20] Liu DJ, He XQ, Gao ZG, Duan Q, Zhou FG. Nonlinear and optical limiting properties of tetra tert-butylnaphthalocyanine lead. Acta Chimica Sinica 2008; 66:563–6.
[21] Cai X, Zhang Y, Zhang X, Jiang J. Structures and properties of 2,3,9,10,16,17,23,24-octasubstituted phthalocyaninato-lead complexes: the substitutional effect study on the basis of density functional theory calculations. Journal of Molecular Structure Theochem 2006;801:71–80.
[22] Zhang Y, Zhang X, Liu Z, Xu H, Jiang J. Comparative density functional theory study of the structures and properties of metallophthalocyanines of group IV B. Vibrational Spectroscopy 2006;40:289–98.
[23] Zhang Y, Zhang X, Liu Z, Bian Y, Jiang J. Structures and properties of 1,8,15,22-Tetrasubstituted phthalocyaninato-lead complexes: the substitutional effect study based on density functional theory calculations. Journal of Physical Chemistry A 2005;109:6363–70.
[24] Piechocki C, Boulou JC, Simon J. Annelides. 22. Discotic mesogens possessing an electrical dipole-moment perpendicular to the molecular plane – Synthesis and mesomorphic properties. Molecular Crystals and Liquid Crystals 1987;149:115–20.
[25] Hanack M, Beck A, Lehmann H. Synthesis of liquid crystalline phthalocyanines. Synthesis 1987;8:703–5.
[26] Ford WT, Sumner L, Zhu W, Chang YH, Um PJ, Choi KH, et al. Liquid-crystalline octa-(2-ethylhexyloxy) platinum and lead phthalocyanines. New Journal of Chemistry 1994;18:495–505.
[27] Weber P, Guillon D, Skoulios A. Antiferroelectric stacking in lead phthalocyanine columnar mesophases. Journal of Physical Chemistry 1987;91:2242–3.
[28] Hanack M, Gül A, Hirsch A, Mandal BK, Subramanian LR, Witke E. Synthesis and characterization of soluble phthalocyanines. Molecular Crystals and Liquid Crystals 1990;187:365–82.
[29] Engel MK, Bassoul P, Bosio L, Lehmann H, Hanack M, Simon J. Mesomorphic molecular materials. Influence of chain length on the structural properties of octa-alkyl substituted phthalocyanines. Liquid Crystals 1993;15:709–22.
[30] McKeown NB. Phthalocyanine materials: synthesis, structure, function. Cambridge: Cambridge University Press; 1998.
[31] Masurel D, Sirlin C, Simon J. Annelides. 21. Highly ordered columnar liquid-crystal obtained from new octasubstituted phthalocyanine mesogen. New Journal of Chemistry 1987;11:455–6.
[32] Ohta K, Jacquemin L, Sirlin C, Bosio L, Simon J. Influence of the nature of the side-chains on the mesomorphic properties of octasubstituted phthalocyanine derivatives - Annelides-XXIX. New Journal of Chemistry 1988;12:751–4.
[33] Adam D, Schuhmacher P, Simmerer J, Haissling L, Siemensmeyer K, Etzbach K, et al. Fast photoconduction in the highly ordered columnar phase of a discotic liquid crystal. Nature 1994;371:141–3.
[34] Basova TV, Gürek AG, Atilla D, Hassan A, Ahsen V. Synthesis and characterization of new mesomorphic octakis(alkylthio)-substituted lead phthalocyanines and their films. Polyhedron 2007;26:5045–52.
[35] Gürek AG, Ahsen V, Heineman F, Zugenmaier P. Synthesis and liquid-crystalline behaviour of tetrakis- and octakis-(13,17-dioxanonacosane-15-

sulfhanyl) phthalocyanines. Molecular Crystals and Liquid Crystals 2000;338:75–97.
[36] Atilla D, Aslıbay G, Gürek AG, Can H, Ahsen V. Synthesis and characterization of liquid crystalline tetra- and octa-substituted novel phthalocyanines. Polyhedron 2007;26:1061–9.
[37] Gürol I, Ahsen V, Bekaroğlu Ö. Synthesis of tetraalkylthio-substituted phthalocyanines and their complexation with Ag(I) and Pd(II). Journal of the Chemical Society. Dalton Transactions; 1994:497–500.
[38] Ban K, Nishizawa K, Ohta K, Shirai H. Discotic liquid crystals of transition metal complexes 27: supramolecular structure of liquid crystalline octakis-alkylthiophthalocyanines and their copper complexes. Journal of Materials Chemistry 2000;10:1083–90.
[39] Perrin DD, Armarego WL. Purification of laboratory chemicals. Oxford: Pergamon Press; 1989.
[40] Becke AD. Density-functional thermochemistry.3. The role of exact exchange. Journal of Chemical Physics 1993;98:5648–52.
[41] Hay PJ, Wadt WR. Ab initio effect core potentials for molecular calculations – Potentials for K to au including the outermost core orbitals. Journal of Chemical Physics 1985;82:299–310.
[42] Frisch MJ, Trucks GW, Schlegel HB, Scuseria GE, Robb MA, Cheeseman JR, et al. Gaussian 03, Revision E.01. Wallingford CT: Gaussian, Inc.; 2004.
[43] Piechocki C, Simon J, Skoulios A, Gullion D, Weber P. Discotic mesophases obtained from substituted metallophthalocyanines – Towards liquid-crystalline one-dimensional conductors. Journal of the American Chemical Society 1982;104:5245–7.
[44] van der Pol JF, Neeleman E, Zwikker JW, Nolte RJM, Drenth W, Aerts J, et al. Homologous series of liquid-crystalline metal free and copper octa-*n*-alkoxyphthalocyanines. Liquid Crystals 1989;6:577–92.
[45] Ukei K. Lead phthalocyanine. Acta Crystallographica Section B 1973;29: 2290–2.
[46] Simon J, Bassoul P. Phthalocyanine based liquid crystals: towards Submicronic devices. In: Leznof CC, Lever ABP, editors. Phthalocyanines, properties and application, vol. 2. Weinheim, Germany: VCH; 1993. p. 22.
[47] Mizuguchi JRG, Karfunkel HR. Solid-state spectra of titanylphthalocyanine as viewed from molecular distortion. Journal of Physical Chemistry 1995; 99:16217–27.
[48] Miyamoto A, Nichogi K, Taomoto A, Nambu T, Murakami M. Structural control of evaporated lead-phthalocyanine films. Thin Solid Films 1995;256:64–7.
[49] Coppede N, Toccoli T, Pallaoro A, Siviero F, Walzer K, Castriota M, et al. Polymorphism and phase control in titanyl phthalocyanine thin films grown by supersonic molecular beam deposition. Journal of Physical Chemistry A 2007;111:12550–8.
[50] Kasha M, Rawls HR, El-Bayoumi MA. The exciton model in molecular spectroscopy. Pure and Applied Chemistry 1965;11:371–92.
[51] Hatsusaka K, Ohta K, Yamamoto I, Shirai H. Discotic liquid crystals of transition metal complexes, Part 30: spontaneous uniform homeotropic alignment of octakis(dialkoxyphenoxy) phthalocyaninatocopper(II) complexes. Journal of Materials Chemistry 2001;11:423–33.
[52] Cook MJ, Chambrier I. Phthalocyanine thin films: deposition and structural studies. In: Kadish KM, Smith R, Guilard R, editors. Applications of phthalocyanines. The Porphyrin Handbook, vol. 17. San Diego, CA: Academic Press; 2003. p. 37–176.
[53] Hassan BM, Li H, McKeown NB. The control of molecular self-association in spin-coated films of substituted phthalocyanines. Journal of Materials Chemistry 2000;10:39–45.
[54] Basova TV, Kolesov BA, Gürek AG, Ahsen V. Raman polarization study of the film orientation of liquid crystalline NiPc. Thin Solid Films 2001;385:246–51.
[55] Basova T, Gürek AG, Ahsen V. Investigation of liquid-crystalline behavior of nickel octakisalkylthiophthalocyanines and orientation of their films. Materials Science and Engineering C 2002;22:99–104.
[56] Battisti D, Aroca R, Loutfy RO. From molecules to thin solid films: vibrational characterization of evaporated organic films. Chemistry of Materials 1989;1:124–8.
[57] Del Cano T, Parra V, Rodriguez-Mendez ML, Aroca RF, De Saja JA. Characterization of evaporated trivalente and tetravalente phthalocaynines films: different degree of organization. Applied Surface Science 2005; 246:327–33.
[58] de Cupere V, Tant J, Viville P, Lazzaroni R, Osikowicz W, Salaneck WR, et al. Effect of interfaces on the alignment of a discotic liquid–crystalline phthalocyanine. Langmuir 2006;22:7798–806.
[59] Basova TV, Durmuş M, Gürek AG, Ahsen V, Hassan A. Effect of interface on the orientation of the liquid crystalline nickel phthalocyanine films. Journal of Physical Chemistry C 2009;113:19251–7.
[60] Basova T, Koltsov E, Hassan AK, Ray AK, Gürek AG, Ahsen V. Effects of structural reorganization in phthalocyanine films on their electrical properties. Materials Chemistry and Physics 2006;96:129–35.